Journal of Fluorine Chemistry 188 (2016) 177–184

Contents lists available at ScienceDirect

Journal of Fluorine Chemistry

journal homepage: www.elsevier.com/locate/fluor

Synthesis, NMR, photoluminescence studies and intramolecular energy transfer process of europium(III) complexes

Manju Bala, Satish Kumar, Rekha Devi, V.B. Taxak, Priti Boora, S.P. Khatkar*

Department of Chemistry, Maharshi Dayanand University, Rohtak 124001, Haryana, India

ARTICLE INFO

Article history:
Received 18 May 2016
Received in revised form 13 July 2016
Accepted 15 July 2016
Available online 16 July 2016

Keywords:
Luminescence properties
NMR shift reagents
Emission spectra
Judd-Ofelt intensity parameter

ABSTRACT

The studies related to the synthesis and luminescence properties of five europium(III) complexes of the type [Eu(OFHD)L] where OFHD is deprotonated 1,1,1,5,5,6,6,6-octafluorohexane-2,4-dione and L is H_2O (**C1**), 2,2′-biquinoline (**C2**), neocuproine (**C3**), 1,10-phenanthroline (**C4**) and 2,2′- bipyridyl (**C5**) are reported in the present communication. The synthesized complexes were investigated by means of elemental analysis, IR, ^1H NMR, UV–vis spectroscopy and TGA techniques. The high fluorination in the complexes makes them best candidates of NMR shift reagents to resolve the spectra as revealed in ^1H NMR study. The excitation and emission spectra of complexes in solid state were investigated in detail. Further, on the basis of emission spectra, the CIE color coordinates (x and y), luminescence decay time (τ), radiative decay rate (A_{rad}), nonradiative rate (A_{nrad}), quantum efficiency (η) and Judd-Ofelt intensity parameter (Ω_2) were calculated and analyzed. The interaction of lowest triplet levels of ligands with the emitting levels of europium(III) ion is represented by proposed intramolecular energy transfer mechanism. The beauty of these complexes is that they can be used as NMR shift reagents and are of particular interest in the field of light emitting materials.

1. Introduction

The investigations of lanthanide (Ln) ion complexes functionallized with fluorinated β-diketone ligands have mesmerised the researchers, making it the most fascinating field of study. These complexes possess unique properties by virtue of which they find applications in the field of organic light emitting devices (OLEDs), optical fibers, lasers [1–3], chemical and biological sensors [4,5]. The most potential chemical property of fluorinated tris Ln(III) complexes i.e. Lewis acidity is due to presence of more fluorine atom which permits them best candidature as NMR shift reagent in spectral simplification [6–8]. Since the 4f electrons of Ln ion are shielded from ligand environment by 5s and 5p electrons, the narrow emission peaks are noticed in luminescence spectra. The most significant aspect of luminescence of Ln(III) complexes is associated with Laporte-forbidden f-f transitions having weak dipole strength, which are accountable for low molar extinction coefficient, resulting into impracticable direct excitation of metal ion. To solve the aforementioned difficulty, the Ln(III) ion is encapsulated with light harvesting chromophoric organic moeity. These organic moieties have high absorption coefficient over a wide range of wavelength, which is advantageous in strong absorption of energy and subsequent transfer of the absorbed energy to Ln(III) ion, thus acting as antenna. There are number of chromophoric organic moieties, however the fluorinated β-diketone are of peculiar interest because of fluorine substituents, which facilitate spin-orbit coupling via heavy atom effect and promote intersystem crossing of sensitization process [9–13]. As we know that the fluorine atom is heavier than hydrogen atom so, the vibration energy of the C-F bond is lower than that of C—H bond. These lower energy frequency C-F oscillators reduce the energy loss during non-radiative decay process. Additionally, it also increases the acidity of the central Ln(III) ion and creates an easily available complexing site for the N,N-donor ancillary ligands. In this way, Ln(III) ion saturates their coordinative sites and prevents the inner coordination sphere from O—H, C—H and N—H higher energy oscillators of solvent molecules that are responsible for quenching of Ln(III) excited state by non-radiative decay process [14]. The coordination of ancillary ligands also provides rigidity and stability to the coordination sphere and diminishes the non-radiative decay [15]. We have chosen four N,N-donor neutral ancillary ligands comprising of two different basic frameworks i.e. one similar to bipy while the other is similar to phen. All the characteristic features of fluorinated β-diketone and ancillary

---

* Corresponding Author.
E-mail address: s_khatkar@rediffmail.com (S.P. Khatkar).

http://dx.doi.org/10.1016/j.jfluchem.2016.07.005
0022-1139/

Table 1
The elemental analytical data of europium(III) complexes **C1–C5.**

Complexes	C(%) found (cal.)	H(%) found (cal.)	N(%) found (cal.)	Eu(%) found (cal.)
HOFHD	27.82 (27.90)	0.75 (0.77)	–	–
C1	22.45 (22.52)	0.70 (0.72)	–	15.68 (15.84)
C2	36.55 (36.64)	1.22 (1.27)	2.25 (2.37)	12.78 (12.89)
C3	33.87 (33.95)	1.28 (1.32)	2.40 (2.47)	13.35 (13.43)
C4	32.58 (32.63)	0.95 (0.99)	2.49 (2.53)	13.72 (13.78)
C5	31.08 (31.13)	1.00 (1.01)	2.48 (2.59)	14.02 (14.08)

ligands greatly enhance the photoluminescence of Ln(III) metal complexes.

In the present communication, we have successfully synthesized five new europium(III) complexes and characterized with various techniques. A detailed study of photophysical properties has been done in order to explore the excitation and emission spectra, CIE coordinates, luminescence decay curves, radiative decay rate (A$_{rad}$), nonradiative rate (A$_{nrad}$), quantum efficiency (η) and Judd-Ofelt intensity parameter (Ω_2). Furthermore, the intramolecular energy transfer process in complexes has been examined by the proposed energy transfer mechanism.

2. Results and discussion

The results of elemental analyses and complexometric titration of europium ion with EDTA are summarized in Table 1. Table 1 clearly shows the conformity between theoretical values and experimental values which indicates successful synthesis of ligand and complexes. The complexes were stable in normal atmospheric conditions and amorphous in nature.

2.1. UV–vis spectra

The UV–vis absorption spectra of ligand and their complexes are depicted in Fig. 1. The maximum absorption of both ligand and complexes was located around 325 nm, showing that singlet energy of the ligand was not affected by coordination of europium ion. These absorption bands were attributed to π-π* transition of ligand. Fig. 1 shows that ligand exhibits absorption over wide range of wavelengths, as compared to complexes and transfer the absorbed energy to the europium ion in an effective way. The spectra were slightly blurred out due to the solvent effect [16].

2.2. NMR spectra

The ^{1}H NMR spectra of paramagnetic complexes showed some interesting changes as compared to spectra of ligands. Some downfield as well as upfield shifts in spectra of complexes were observed due to large magnetic anisotropy of europium. The spectrum of ligand showed the signal of enolic —OH proton at 15.30 ppm. This signal disappeared in spectra of complexes, manifesting the coordination of ligand to the metal ion through enolic form. The singlet of methine (=C—H) proton in spectrum of ligand shifted to upfield in the spectra of complexes as the OFHD binds with Eu^{3+} ion ligated by bipy or phen. This shift also occurred due to the high polarization of Eu^{3+} ion after withdrawing the electron density from ancillary ligand, hence, some electron density shifted from Eu^{3+} ion to the OFHD ligand which can be easily accomodated by highly electronegtive fluorine atoms present in the OFHD. Consequently, the aromatic signals of ancillary ligands exhibited remarkable downfield shift in spectra of complexes. The NMR spectra of HOFHD ligand and complexes of phen and bipy ancillary ligands of different basic frameworks i.e. **C4** and **C5** complexes are depicted in Figs. 2 and 3 [17,18].

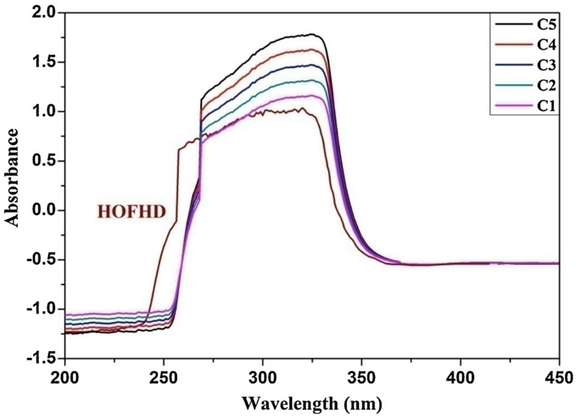

Fig. 1. The UV–vis absorption spectra of HOFHD ligand and **C1–C5** europium(III) complexes in DMSO solvent (1×10^{-5} mol/L).

The peak broadening effect could be observed due to presence of protons in close proximity of europium(III) ion and absence of spin-spin splitting. Among the complexes, only **C5** complex showed broad signals due to coordination of bipy which leads to disappearing of spin-spin splitting. This demonstrated that both ends of bipy firmly coordinated to the europium(III) ion [17]. Other complexes showed no signal broadening, therefore these were more applicable in state of presence of spin-spin splitting in complexes, hence used as NMR shift reagents to solve the spectra.

2.3. IR spectra

Fig. 4 depicts the IR spectra of ligand and complexes, the important IR bands are tabulated in Table 2. The complexes showed almost similar IR spectra, suggesting similar modes of binding of ligand in all the complexes. These spectra differ from the spectrum of free ligand. As we know that the stretching vibration of >C=O group is highly sensitive to complexation. The IR spectrum of ligand exhibited the absorption bands at 1718 cm^{-1} and 1606 cm^{-1}, ascribed to the stretching vibrations of >C=O and C=C respectively. These two bands shift to 1659–1648 cm^{-1} and 1546–1500 cm^{-1} respectively in the spectra of complexes which make it clear that the >C=O group was involved in complexation. This is further confirmed by the bands of Eu-O vibrations in region 471–462 cm^{-1} which came into existence in the spectra of complexes only. Two new bands in the region 1597–1592 cm^{-1} and 536–534 cm^{-1} appeared due to coordination of ancillary ligands in **C2**–**C5** complexes corresponding to C=N and Eu-N stretching vibrations respectively. The spectrum of ligand displayed a broad band of enolic —OH at 3270 cm^{-1}. On the other hand, a broad band of —OH vibration of water molecules at 3429 cm^{-1} was observed in spectra of C1 complex only which disappeared in **C2–**C5, suggesting the successful substitution of solvent molecule by ancillary ligands. The strong absorption band of C—F stretching vibrations in the region 1203–1196 cm^{-1} were common to all complexes as well as ligand and exhibited no change in the values which showed that C-F bond did not participate in coordination process.

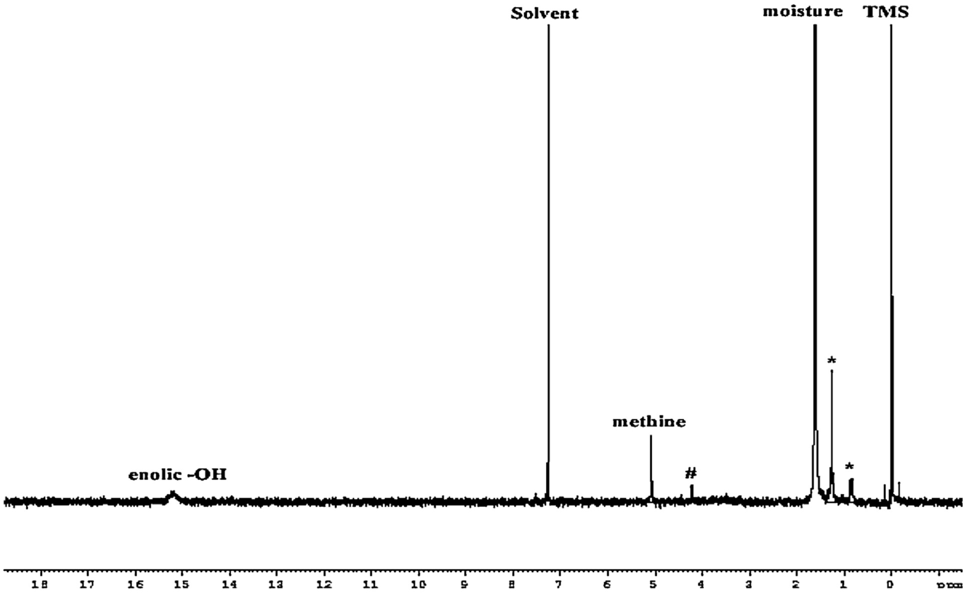

Fig. 2. The ^{1}H NMR spectra of HOFHD ligand. *Impurity and # signal for —CH_2 protons of keto form.

2.4. Thermal analysis

The thermal analysis of the complexes by their TG-DTG thermograms were carried out under dinitrogen atmosphere at a heating rate of 20 °C/min. All the complexes showed almost similar thermal behavior and were stable at about 190 °C temperature [18]. The **C5** complex was selected as representative of all complexe as depicted in Fig. 5 to illustrate the decomposition pattern. The first mass loss of 2.2% upto 118 °C was observed due to moisture present in complex. The second large step of mass loss of 85.7% between 190 and 356 °C temperatures corresponds to the removal of three OFHD and one bipy molecules. At last, europium oxide remained as final product.

2.5. Luminescence features

In order to investigate the photoluminescence properties of **C1–C5** europium(III) ion complexes, the excitation and emission spectra were measured in solid state at room temperature as displayed in Figs. 6 and 7. The excitation spectra of complexes were recorded by monitoring the emission maxima of $^{5}D_0$-$^{7}F_2$ transition. A broad band centred at 351 nm in the range of 200–500 nm prevailed in the spectra of complexes, ascribed to π-π* transition of ligand. It also indicated that the ligands efficiently sensitized the europium ion by transferring the energy.

Under the UV irradiation of 351 nm, the emission spectra of complexes exhibited characteristic peaks of Eu^{3+} ion originating from electronic transition from $^{5}D_{0,1}$ to $^{7}F_{0,1,2}$ levels. No ligand based emission was observed in emission spectra of complexes, suggesting the complete transfer of absorbed energy of ligand to the metal ion. The most intense $^{5}D_0$-$^{7}F_2$ transition at 616 nm was an induced electric dipole transition which was highly sensitive to its coordination environment and amenable for red emission of the complexes. The $^{5}D_0$-$^{7}F_1$ transition around 591–592 nm was magnetic dipole transition which was insensitive to its coordination environment. On the contrary, the $^{5}D_0$-$^{7}F_0$ transition at 580 nm was forbidden both in electric as well as magnetic dipole. The values of intensity ration (I_{02}/I_{01}) of $^{5}D_0$-$^{7}F_2$ to $^{5}D_0$-$^{7}F_1$

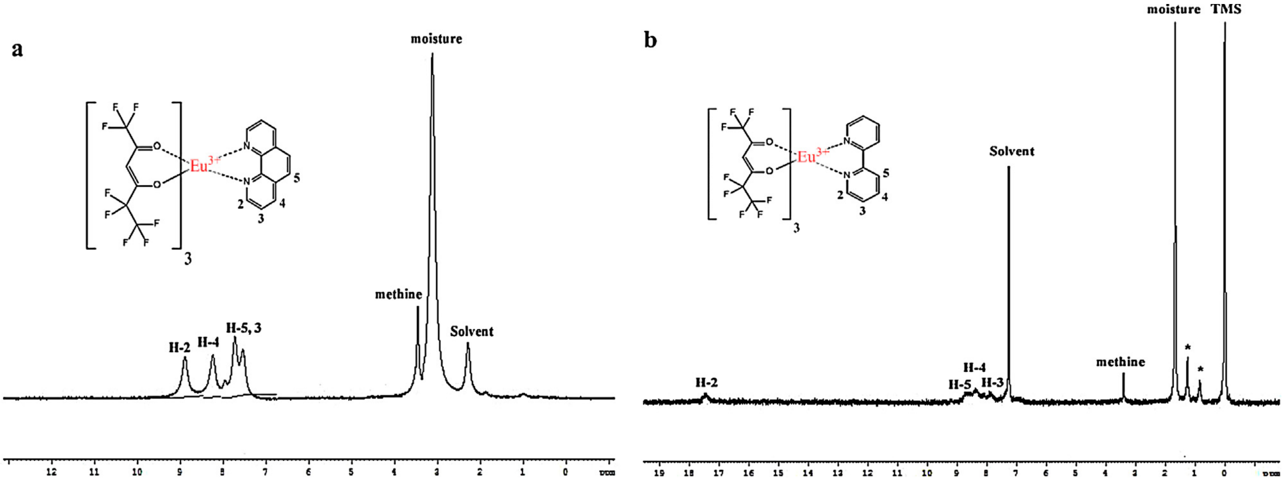

Fig. 3. The ^{1}H NMR spectra of **C4** (a) and **C5** (b) complexes.

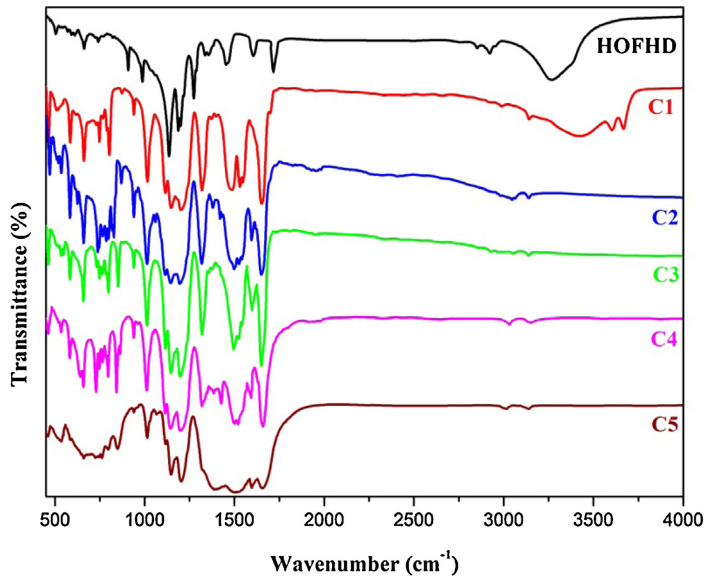

Fig. 4. IR absorption spectra of HOFHD ligand and its **C1–C5** complexes.

Table 2
The IR characteristics bands (cm^{-1}) of ligand and its europium complexes.

Complexes	ν(O—H)	ν(C=O)	ν(C=N)	ν(C=C)	ν(C—F)	ν(Eu—N)	ν(Eu—O)
HOFHD	3270 (b)	1718 (s)	–	1606 (s)	1200 (s)	–	–
C1	3429 (b)	1651 (s)	–	1546 (s)	1202 (s)	–	463 (m)
C2	–	1648 (s)	1595 (s)	1541 (s)	1196 (s)	536 (s)	471 (m)
C3	–	1651 (s)	1597 (s)	1540 (s)	1198 (s)	535 (m)	462 (w)
C4	–	1659 (s)	1592 (s)	1520 (s)	1199 (s)	534 (s)	463 (m)
C5	–	1656 (s)	1595 (s)	1500 (s)	1203 (s)	535 (s)	462 (m)

b = broad, s = strong, m = medium, w = weak.

transition are given in Table 3, suggesting that the europium ion was engaged in non-centrosymmetric position in complexes [19,20]. Only one peak for $^5D_0$-$^7F_0$ and $^5D_0$-$^7F_1$ transitions was noticed in spectra pointing towards the presence of single chemical environment around the europium(III) ion. The analysis of emission spectra clearly revealed that the introduction of ancillary ligands in **C2–C5** complexes enhanced the luminescence intensity, assigned to the synergistic effect of these ancillary ligands. It can be seen that the ancillary ligands could sensitize the luminescence intensity of europium ion. Hence we obtained the higher luminescence intensity of **C2–C5** complexes as compared to **C1** complex. On the other hand, the O—H oscillators of water molecule in **C1** complex quenched the luminescence intensity by increase the non-radiative decay. The nature of the ancillary ligands controlled the order of luminescence emission intensity in the **C2–C5** complexes. As we have chosen four ancillary ligands which belong to two different basic framework groups i.e one framework group have bipy and biq while other have phen and neo. The steric effect in case of biq and neo ligands makes them less intense in their respective groups. The luminescence intensity order of bipy and phen can be explained on the basis of energy gap ΔE (T_1-M^{3+}) value. This gap was found to be the most appropriate match in bipy and hence has highest emission intensity, also explained elaborately in energy transfer mechanism.

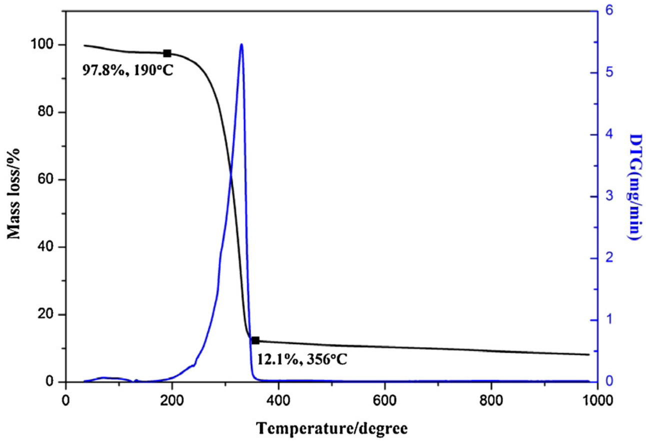

Fig. 5. TG-DTG curves of **C5** complex under dinitrogen atmosphere.

The CIE (Commission Internationale de Eclairage) color coordinates (x and y) of complexes were estimated from emission spectra and their values are listed in Table. 3. CIE coordinates of complexes fell under the red region of chromaticity diagram as shown in Fig. 8 and are close to the standard red color values of SMPTE (Society of Motion Picture and Television, x = 0.63, y = 0.34) and EBU (European Broadcasting Union, x = 0.64, y = 0.33).

2.6. Luminescence decay time (τ), quantum efficiency (η) and Judd-Ofelt analysis

The luminescence decay curves of $^5D_0$ excited state of Eu(III) ion in complexes were examined by monitoring the emission of

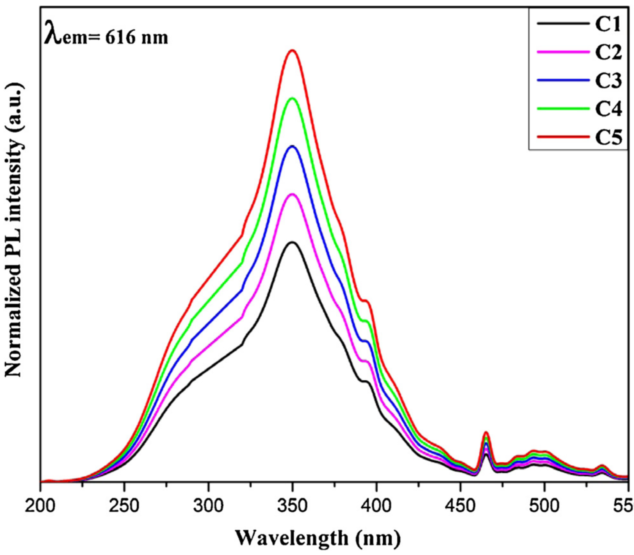

Fig. 6. Solid state excitation spectra of **C1–C5** complexes monitored at 616 nm at room temperature.

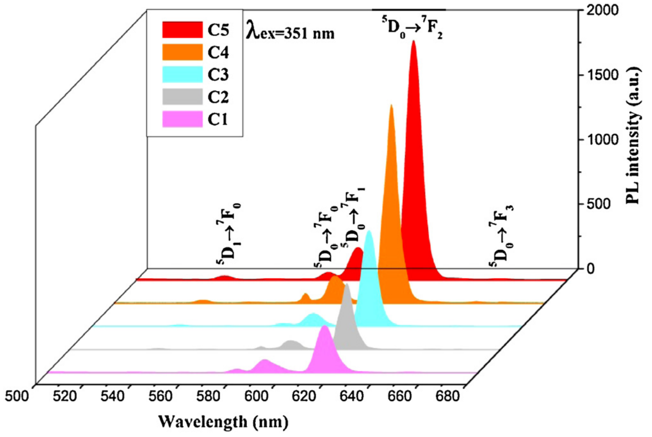

Fig. 7. Solid state emission spectra of **C1–C5** complexes excited at 351 nm.

Table 3
The luminescence data of **C1–C5** complexes.[a]

Systems	C1	C2	C3	C4	C5
x and y color coordinates	0.5264, 0.2913	0.5343, 0.3142	0.5928, 0.3183	0.6212, 0.3322	0.6471, 0.3524
ν_{00} (cm^{-1})	17241	17241	17241	17241	17241
ν_{01} (cm^{-1})	16920	16891	16891	16891	16891
ν_{02} (cm^{-1})	16233	16233	16233	16233	16233
I_{00}	30	25	25	75	60
I_{01}	100	75	96	208	250
I_{02}	350	520	616	1530	1856
I_{02}/I_{01}	3.5	6.93	7.68	7.35	7.42
A_{00} (s^{-1})	14.72	16.32	12.75	17.66	11.75
A_{01} (s^{-1})	50.0	50.0	50.0	50.0	50.0
A_{02} (s^{-1})	182.40	360.71	400.0	382.70	386.24
τ (ms)	0.36	0.44	0.75	0.87	0.95
A_{rad} (s^{-1})	247.12	427.03	462.75	450.36	448.0
A_{nrad} (s^{-1})	2530.65	1845.69	870.58	699.06	604.63
η (%)	8.89	18.78	34.70	39.18	42.56
Ω_2 (x10^{-20})	4.08	8.08	8.96	8.56	8.65

[a] The intensity of $^5D_0$-$^7F_3$ transition is very low so their corresponding ν_{03} and I_{03} are neglected.

$^5D_0$-$^7F_2$ transition at 616 nm excited at 351 nm as shown in Fig. 9. These curves fitted with a single exponential function, suggesting that europium(III) ion was located at the same parity site in the complexes. The luminescence decay time values were calculated from fitting of decay curves and are summarized in Table. 3. It is seen that the decay time of **C1** complex was lower than that of **C2–C5** complexes because the former complex had O—H quencher of water molecule while in latter complexes water molecules are substituted by ancillary ligands. Similar results were also obtained in case of quantum efficiency (η).

The quantum efficiency of the $^5D_0$ excited state was determined from emission spectra and decay time of the complexes. It expressed the competition between radiative and nonradiative process as given below [21,22]:

$$\eta = A_{rad}/A_{rad} + A_{nrad} \tag{1}$$

The radiative and nonradiative processes are represented by the rate constant A_{rad} and A_{nrad} respectively. It was considered that only these processes participate in the depopulation of $^5D_0$ excited state and are related with luminescence decay time by the Eq. (2).

$$\tau = (A_{rad} + A_{nrad})^{-1} \tag{2}$$

$$A_{rad} = A_{01}\frac{\nu_{01}}{I_{01}}\sum_{j=0}^{4}\frac{I_{0J}}{\nu_{0J}} = \sum\nolimits_j A_{0J} \tag{3}$$

Here, A_{rad} was obtained by summation of all radiative rates A_{0J} for each characteristics transitions ($^5D_0\rightarrow{}^7F_{0\text{-}J}$) of europium ion as shown in Eq. (3). A_{0J} was calculated according to Eq. (4) [23,24]. The transitions which were not detected in emission spectra such as $^5D_0\rightarrow{}^7F_{4\text{-}6}$, can be neglected as they were not involved in depopulation process. Since $^5D_0\rightarrow{}^7F_1$ transition was magnetic dipole transition and insensitive to chemical environment around europium ion, it can be used as an internal reference for whole spectrum.

$$A_{0J} = A_{01}(I_{0J}/I_{01})(\nu_{01}/\nu_{0J}) \tag{4}$$

Here, A_{01} is the Einstein's coefficient of spontaneous emission between the $^5D_0$ and $^7F_1$ energy states. The value of A_{01} has to be taken 14.65 s^{-1} in vacuum while 50 s^{-1} approximately ($A_{01} = n^3 A_{01vac}$) in air, when an average index of refraction (n) is considered to be 1.506 [25]. The $\nu\nu_{01}$ and ν_{0J} are energy barycenter of $^5D_0\rightarrow{}^7F_1$ and $^5D_0\rightarrow{}^7F_J$ transition respectively with I_{01} and I_{0J} as integrated intensities respectively. The quantum efficiency of all the complexes was calculated using above equations and the data are tabulated in Table 3. It is concluded that value of η depends mainly on decay time and ratio of I_{02}/I_{01}, higher the value of decay time and I_{02}/I_{01} ratio, higher will be the quantum efficiency. The lower value of η in **C1** as compared to **C2–C5** complexes may be explained on the basis of existance of more nonradiative process which comes into existance due to —OH vibronic coupling of water molecules in former complex.

The Judd-Ofelt theory is implemented to analyze the possible structural changes around europium ion and line strength of an electrical dipole transition in the form of Judd-Ofelt intensity parameters Ω_2 and Ω_4. Out of these parameters, Ω_2 parameter is highly sensitive to the symmetry and sequence of ligand field. The large value of Ω_2 parameter gives rise to non-symmetric environment around europium ion and faster radiation rate (A_{rad}) [26].

As discussed earlier, the emission transitions such as $^5D_0\rightarrow{}^7F_{0,3,5}$ were forbidden in both electric and magnetic dipole transition while the $^5D_0\rightarrow{}^7F_1$ transition was magnetic dipole transition. The $^5D_0\rightarrow{}^7F_{2,4}$ transitions are contributing towards

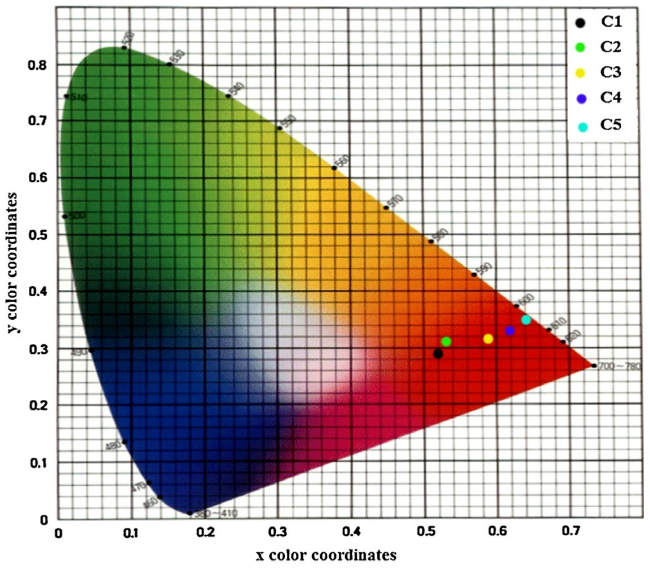

Fig. 8. The CIE color coordinates of **C1–C5** complexes.

electric dipole so, the Ω_2 and Ω_4 parameters are estimated according to Eq. (5) as expressed below [27].

$$\Omega_\lambda = 3\hbar c^3 A_{0j}/4e^2\omega^3\chi < 5_{D_0}|U^{(\lambda)}|7_{F_j} >^2 \qquad (5)$$

Here, ħ is taken as Planck's constant over 2π, c is velocity of light, e is the electronic charge, ω is angular frequency of electronic transition, χ is Lorenz local field correction $[n^2(n^2+2)^2/9]$in which 1.5 average refractive index is used and $< 5_{D_0}|U^{(\lambda)}|7_{F_j} >^2$ is taken as 0.0032, representing the square reduced matrix elements [28]. The Ω_2 intensity parameter for all the complexes is shown in Table 3 and Ω_4 parameter was not calculated because $^5D_0 \rightarrow {}^7F_4$ transition could not be experimentally detected. It was noticed that the **C5** complex had relatively higher value of Ω_2 as a consequence of hypersensitive behavior of $^5D_0 \rightarrow {}^7F_2$ transition, reflecting the most polarizable chemical environment around Eu^{3+} in complex.

2.7. Energy transfer mechanism

The proposed channel for the intramolecular energy transfer process is shown in Fig. 9. The energy transfer predominantly occured between triplet energy level (T_1) of ligand to the nearby emitting level (M^{3+}) of europium ion. The triplet level of fluorinated β-diketone was more favourable for efficient energy transfer to the metal ion because the fluorine atom can lower the triplet energy level which make it suitable match with the emitting level of metal ion. The singlet (S_1; 27397 cm^{-1}) and triplet (T_1; 22371 cm^{-1}) levels of OFHD ligand were calculated from the UV–vis absorption edge wavelength of spectra (Fig. 1) and shortest phosphorescence emission wavelength of its corresponding gadolinium complex (**G1**) as depicted in Fig. S1. In the literature, it can be observed that the triplet levels of ancillary ligands are nearly close to one another, therefore, the lowest singlet and triplet levels of bipy (S_1; 29900 cm^{-1}, T_1; 22900 cm^{-1}) and phen (S_1; 31000 cm^{-1}, T_1; 22100 cm^{-1}) ligands were estimated, which matched with the literature [29,30]. But, the energy gap (T_1-M^{3+}) should be appropriate for efficient energy transfer, it should be neither too large nor too small. Latva et al. initially stated that this energy gap $\Delta E(T_1\text{-}M^{3+})$ should be in 2000–5000 cm^{-1} range for efficient energy transfer process [31]. The value of energy gap (ΔE) for HOFHD, bipy and phen were found to be 3750 cm^{-1}, 4279 cm^{-1} and 3479 cm^{-1} respectively. It can be seen that the value of energy gap of phen was lower than that of bipy energy gap value which was responsible for small thermally activated M^{3+} to T_1 inverse energy transfer. Hence, the luminescence emission intensity of phen complex was noticed to be lower than that of bipy complex. Furthermore, the prime factor governing the transfer of energy from triplet level of ligand to the emitting levels of the metal ion was energy gap (ΔE), which was found to be most appropriate in case of **C5** complex. Hence, this complex showed maximum luminescence emission intensity as illustrated in the proposed energy transfer mechanism of complexes **C4** and **C5** and respectively represented in Figs. S2 and 10 .

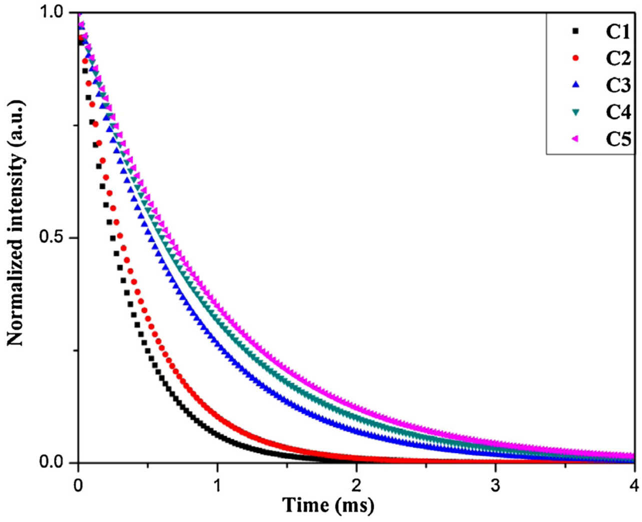

Fig. 9. Luminescence decay curves of **C1–C5** complexes.

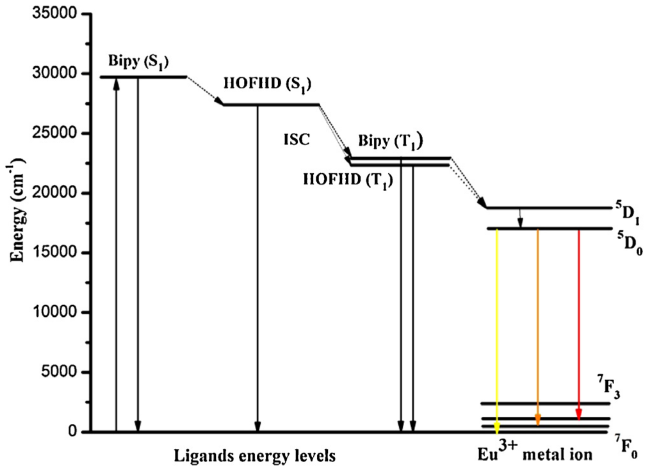

Fig. 10. The proposed energy transfer mechanism in **C5** complex.

3. Conclusion

In this report, a series of five europium complexes with fluorinated β-diketone and ancillary ligands have been succesfully synthesized and well characterized. The ^1H NMR study shows that these complexes can be used as NMR shift reageent to simplify the spectra. The solid state emission spectra excited at 351 nm display characteristic peaks of Eu^{3+} ion and intensity increases as the solvent molecules are substituted by ancillary ligands. The data of quantum efficiency, Ω_2 intensity parameter and decay curves indicate that Eu^{3+} ion is situated in most polarizable chemical environment and acts as one luminescent site. The triplet level of OFHD ligand matches well with emitting level of Eu^{3+} ion, which leads to the efficient energy transfer. The CIE coordinates of complexes fall in deep red region. The excellent results of emission spectra, CIE, decay curves, quantum efficiency and Ω_2 intensity parameter make these complexes best candidates as light emitting materials and also widely applicable as red component in display devices (Scheme 1).

4. Experimental details

4.1. Materials

The lanthanide nitrates i.e. $Eu(NO_3)_3 \cdot 5H_2O$ (99.9%); Gd $(NO_3)_3 \cdot 5H_2O$ (99.9) of high purity and ancillary ligands such as 2,2′-bipyridyl, 1,10-phenanthroline, 2,2′-biquinoline and neocuproine were purchased from Sigma Aldrich and were used as received. The solvents and reagents like sodium methoxide, methylpentafluoropropionate, 1,1,1-trifluoropropane-2-one used in this study were of analytical grade.

4.2. Synthesis of ligand

By using Claisen condensation reaction, the fluorinated β-diketonic ligand 1,1,1,5,5,6,6,6-octafluorohexane-2,4-dione (HOFHD) was synthesized. The synthesis and isolation of ligand demands extra care and attention because high fluorination decreases the intermolecular van der waals forces and H-bonding which lead to high volatility of ligands.

Sodium methoxide (0.2 mol) was added in 150 ml of absolute diethyl ether followed by dropwise slow addition of methylpentafluoropropionate (0.2 mol) in the stirred mixture. Then ethereal solution of 1,1,1-trifluoropropane-2-one (0.2 mol) was added slowly, which resulted into basic solution. The mixture was stirred for about 2 h and allowed to cool for 15 h. The resulting mixture was acidified with sulphuric acid (100 ml, 2 M) with constant stirring. The organic and aqueous phase was formed and latter was separated and washed with fresh diethyl ether. Further, these washings of aqueous layer were added to the organic layer and finally the solution was evaporated. Then resulting solution was vacuum distilled to get the final product [32,33].

4.3. Synthesis of complexes

All five Eu(III) complexes were synthesized adopting identical procedure only differing in addition of ancillary ligands in **C2–C5** complexes. For **C1**, 3.2 mmol of HOFHD in 15 ml solution of methanol was mixed with 10 ml solution of distilled water containing 1.0 mmol of europium nitrate. The resulting mixture was stirred on magnetic stirrer set at temperature around 60 °C. Also the pH of the mixture was adjusted to 6.5 with 0.05 M NaOH solution. The off white precipitates formed were filtered, washed with water followed by methanol and then dried in hot air oven. Similarlly, the $Gd(OFHD)_3(H_2O)_2$ (**G1**) was also prepared to estimate the lowest excited triplet state of OFHD ligand. To synthesize the **C2–C5** complexes, the 1.0 mmol of biq for **C2**, neo for

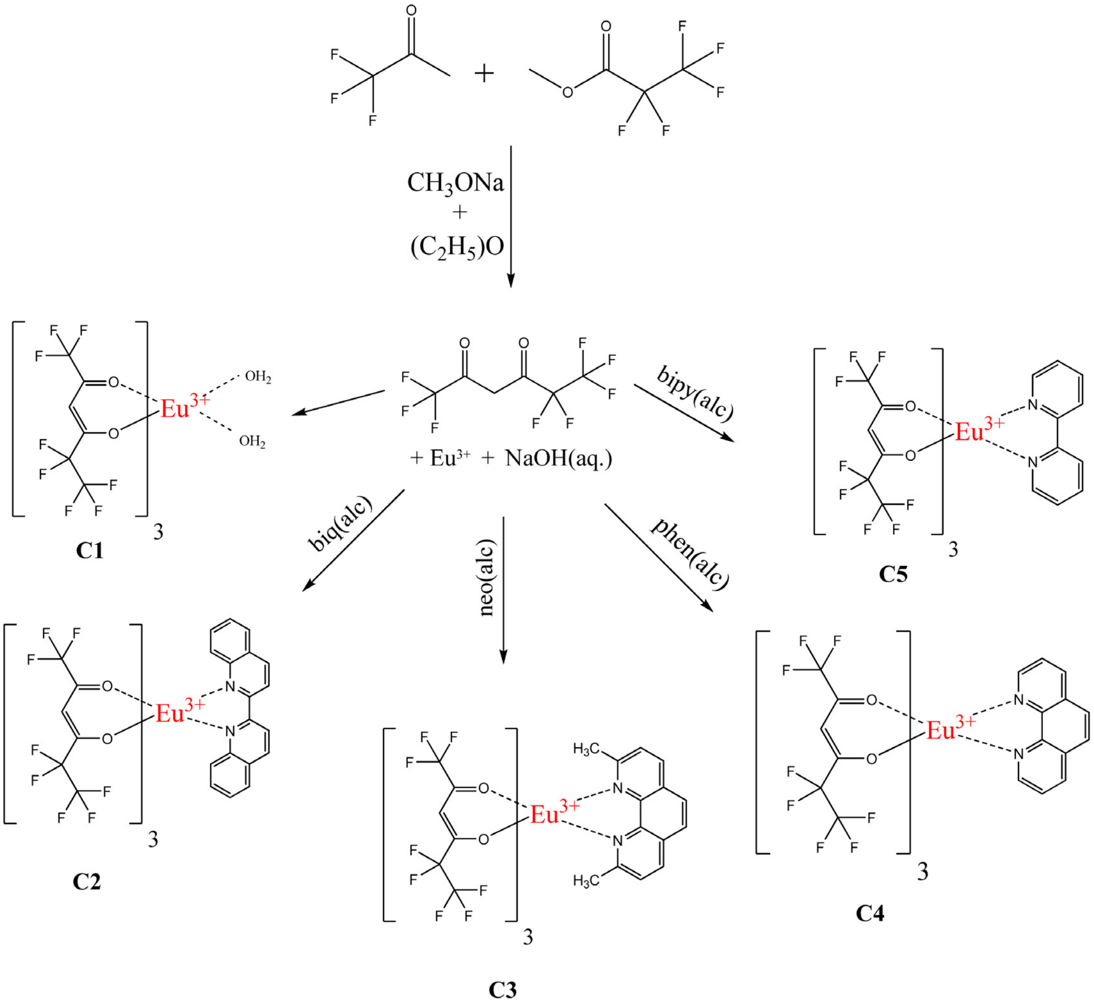

Scheme 1. Pathway for the synthesis of the ligand and its corresponding europium(III) ion complexes.

C3, phen for **C4** and bipy for **C5** in 10 ml methanol was mixed with resulting mixture as prepared for **C1**. Then followed the aforementioned method.

4.4. Physical measurements

Elemental analysis of carbon, hydrogen and nitrogen were carried out with Perkin Elmer 2400 CHN Elemental Analyzer. The europium ion content in complexes was calculated by EDTA (ethylenediaminetetraacetate) complexometric titration method using xylenol orange as an indicator. The infrared (IR) spectra of the complexes in the range of 4000–450 cm^{-1} were measured with Perkin Elmer – Spectrum RX-IFTIR using KBr disks. The ^1H NMR spectra of complexes were recorded on Bruker Avance II 400 NMR spectrometer using tetramethylsilane as a referance. The UV–vis absorption spectra were obtained by Shimadzu-2450 UV–vis spectrophotometer in DMSO solvent. Thermal analyses were performed with Hitachi STA7300 Thermal Analyzer at a heating rate of 20° C/min from ambient temperature to 1000 °C under nitrogen environment. The room temperature excitation and emission spectra of complexes were measured with a Hitachi F-7000 fluorescence spectrophotometer equipped with 150 W xenon lamp in wavelength scan mode at a 240 nm/min scanning speed with 400 PMT. The excitation and emission slit widths were both set to 2.5 nm. In similar way, the luminescence decay curves were determined in time scan mode with the excitation wavelength of 351 nm.

Aknowledgement

This work is supported by CSIR (Council of Science and Industrial Research) of India in the form of senior research fellowship to one of the authors Mrs. Manju Bala (09/382(0155)/2012- EMR-I).

Appendix A. Supplementary data

Supplementary data associated with this article can be found, in the online version, at http://dx.doi.org/10.1016/j.jfluchem.2016.07.005.

References

[1] K. Binnemans, Chem. Rev. 109 (2009) 4283–4374.
[2] K. Kuriki, Y. Koike, Y. Okamoto, Chem. Rev. 102 (2002) 2347–2356.
[3] S. Akerboom, J.J.M.H. van den Elshout, I. Mutikainen, M.A. Siegler, W.-T. Fu, E. Bouwman, Eur. J. Inorg. Chem. 36 (2013) 6137–6146.
[4] M.S. Tremblay, M. Halim, D. Sames, J. Am. Chem. Soc. 129 (2007) 7570–7577.
[5] D. Geißler, S. Stufler, H.-G. Lő hmannsrő ben, N. Hildebrandt, J. Am. Chem. Soc. 135 (2013) 1102–1109.
[6] J.K.M. Sanders, D.H. Williams, J. Chem. Soc. D 7 (1970) 422–423.
[7] J. Briggs, G.H. Frost, F.A. Hart, G.P. Moss, M.L. Staniforth, J. Chem. Soc. D 12 (1970) 749–750.
[8] K. Iftikhar, Polyhedron 15 (1995) 1113–1120.
[9] J.-C.G. Bünzli, C. Piguet, Chem. Soc. Rev. 34 (2005) 1048–1077.
[10] Y. Zheng, J. Lin, Y. Liang, Q. Lin, Y. Yu, Q. Meng, Y. Zhou, S. Wang, H. Wang, H. Zhang, J. Mater. Chem. 11 (2001) 2615–2619.
[11] P. He, H.H. Wang, S.G. Liu, J.X. Shi, G. Wang, M.L. Gong, Inorg. Chem. 48 (2009) 11382–11387.
[12] N.S. Baek, M.K. Nah, Y.H. Kim, H.K. Kim, J. Lumin. 127 (2007) 707–712.
[13] L.-M. Fu, X.-C. Ai, M.-Y. Li, X.-F. Wen, R. Hao, Y.-S. Wu, Y. Wang, J.-P. Zhang, J. Phys. Chem. A 114 (2010) 4494–4500.
[14] P. Lenaerts, K. Driesen, R.V. Deun, K. Binnemans, Chem. Mater. 17 (2005) 2148–2154.
[15] S.I. Weissman, J. Chem. Phys. 10 (1942) 214–217.
[16] J. Yu, R. Deng, L. Sun, Z. Li, H. Zhang, J. Lumin. 131 (2011) 328–335.
[17] K. Iftikhar, Polyhedron 15 (1996) 1113–1120.
[18] Z. Ahmed, K. Iftikhar, Inorg. Chim. Acta. 392 (2012) 165–176.
[20] A.F. Kirby, D. Foster, F.S. Richardson, Chem. Phys. Lett. 95 (1983) 507–512.
[21] E.E.S. Teotonio, J.G.P. Espı'nola, H.F. Brito, O.L. Malta, S.F. Oliveira, D.L.A. de Faria, C.M.S. Izumi, Polyhedron 21 (2002) 1837–1844.
[22] L.D. Carlos, Y. Messaddeq, H.F. Brito, R.A.S. Ferreira, V.Z. Bermudez, S.J.L. Ribeiro, Adv. Mater. 12 (2000) 594–598.
[23] M.H.V. Werts, R.T.F. Jukes, J.W. Verhoeven, Phys. Chem. Chem. Phys. 4 (2002) 1542–1548.
[24] P.C.R. Soares-Santos, H.I.S. Nogueira, V. Félix, M.G.B. Drew, R.A.S. Ferreira, L.D. Carlos, T. Trindale, Chem. Mater. 15 (2003) 100–108.
[25] R.A.S. Ferreira, L.D. Carlos, R.R. Goncalves, S.J.L. Ribeiro, V.Z. Bermudez, Chem. Mater. 13 (2001) 2991–2998.
[26] Y. Li, B. Yan, Dalton Trans. 39 (2010) 2554–2562.
[27] E.E.S. Teotonio, H.F. Brito, M.C.F.C. Felinto, C.A. Kodaira, O.L. Malta, J. Coord. Chem. 56 (2003) 913–921.
[28] C.A. Kodaira, H.F. Brito, M.C.F.C. Felinto, J. Solid State Chem. 171 (2003) 401–407.
[29] D.B. Ambili Raj, B. Francis, M.L.P. Reddy, R.R. Butorac, V.M. Lynch, A.H. Cowley, Inorg. Chem. 49 (2010) 9055–9063.
[30] X. Yu, Q. Su, J. Photochem. Photobiolog. A 155 (2003) 73–78.
[31] M. Latva, H. Takalo, V.M. Mukkala, C. Matachescu, J.C. Rodríguez-Ubis, J. kankare, J. Lumin. 75 (1997) 149–169.
[32] A.-S. Chauvin, F. Gumy, I. Matsubayashi, Y. Hasegawa, J.-C. Bünzli, Eur. J. Inorg. Chem. (2006) 473–480.
[33] (a) K. Iftikhar, M. Sayeed, N. Ahmad, Inorg. Chem. 21 (1982) 80–84.